UPPSALA
UNIVERSITET

ISRN UTH-INGUTB-EX-E-2013/04-SE
Examensarbete 15 hp
Juni 2013

Completion of the software required for a high-temperature DLTS setup

Rasmus Jansson

UPPSALA
UNIVERSITET

Teknisk- naturvetenskaplig fakultet
UTH-enheten

Besöksadress:
Ångströmlaboratoriet
Lägerhyddsvägen 1
Hus 4, Plan 0

Postadress:
Box 536
751 21 Uppsala

Telefon:
018 – 471 30 03

Telefax:
018 – 471 30 00

Hemsida:
http://www.teknat.uu.se/student

Abstract

Completion of the software required for a high-temperature DLTS setup

Rasmus Jansson

The main purpose of this thesis was to examine the communication problems with the DLTS set up in the Division for Electricity at Ångström Laboratory in Uppsala, Sweden, and to make the DLTS software complete. The set up consisted of a C/V meter, a pulse generator, a temperature controller and a PC with a control program written in LabVIEW. It was found that the software had been constructed to fit another set of instruments than the set up currently used at Ångström Laboratory. The task was therefore to properly integrate the correct control commands of those instruments into the software.

Handledare: Markus Gabrysch
Ämnesgranskare: Saman Majdi
Examinator: Nora Masszi
ISRN UTH-INGUTB-EX-E-2013/04-SE
Tryckt av: Uppsala Universitet, Uppsala

Sammanfattning

(a summary in Swedish)

Halvledare används inom flera områden i elektrotekniska sammanhang. Detta för att deras elektriska egenskaper med lätthet kan formas och styras genom en process som kallas dopning. Ett vanligt material med halvledande egenskaper som används för att tillverka olika elektroniska komponenter är kisel och olika föreningar med kisel. Vid sammansättningen (dopningen) av dessa kiselföreningar bildas också defekter i materialet. Dessa defekter kan beskrivas som kemiska orenheter som markant påverkar den elektriska strömmen genom materialet. Defekterna har den egenheten att de fångar upp laddningsbärare, tex elektroner, och för att fria dem krävs en viss mängd energi, i denna rapport används värmeenergi. En metod för att detektera djupa defekter (*på engelska deep-level defects*) i en halvledare är *deep-level transient spectroscopy*, eller kort DLTS. Metoden går ut på att först tömma defekterna, i provet, på de laddningsbärare som erhållit tillräckligt med energi och sedan låta dessa falla tillbaka till defekterna för att sedan utföra en tömning igen. Processen för att fylla defekterna sker relativt snabbt medan för att tömma dem på laddningsbärare sker över en viss tid. Över denna tid kommer kapacitansen i provet att ändras som funktion av tid och det är denna kapacitansändring som genom signalbehandling ger upphov till en DLTS signal.

Detta projekts huvudsyfte var att undersöka problemen med, samt färdigställa, kommunikationen mellan mätinstrumenten och kontrollprogrammet som utgjorde uppställningen för DLTS mätningar på Ångströms Laboratorium i Uppsala. Uppställningen bestod utav en kapacitansmätare, en pulsgenerator, en temperaturkontroll samt en PC med integrerat kontrollprogram utvecklat i programmeringsmiljön LabVIEW. Problemet bestod i att kontrollprogrammet ej hade blivit uppdaterat enligt det instrument som användes på Ångström. Programmet var konstruerat utav en forskningsgrupp i Norge som använde mätinstrument av andra märken och därför skiljde sig de kontrollkommandon som skulle skickas från programmet. Uppgiften bestod alltså av att integrera de korrekta kommandona för uppställningen på Ångström samt se till att kommunikationen fungerade.

Key words: Semiconductors, DLTS, LabVIEW, VISA, GPIB, 488.2

Preface

This thesis had not been finished without Markus Gabrysch's supervision and guidance, nor without Florian Burmeister's support and encouragement during my time with the group.

I also would like to thank my topic examiner Saman Majdi for his determination to always help in all ways possible.

Supervisor: Markus Gabrysch

Topic examiner: Saman Majdi

Examiner: Nora Masszi

Author: Rasmus Jansson

Ångström Laboratory, Uppsala, Sweden, 2013-06

Contents

Abbreviations....1

1 Introduction....2

1.1 Background....2
1.2 Assignment....3

2 Theory....4

2.1 Atomic- & Band structure in solid-state physics....4
2.1.1 Valence band & conduction band....5
2.2 Defects....5
2.2.1 Deep-level defects....6
2.2.2 Traps....6
2.3 Deep-Level Transient Spectroscopy....6
2.3.1 The capacitance transient....7
2.3.2 Window & weighting functions....8
2.3.3 DLTS signal....9
2.4 Analysis of DLTS & Arrhenius plot....11
2.5 LabVIEW....11
2.5.1 VISA/GPIB....13

3 Method....16

3.1 Experimental setup....16
3.2 Implementation....17
3.2.1 Controls....18
3.2.2 Indicators....21

4 Results....23

5 Discussion & Analysis....24

5.1 Communications....24
5.2 Yudian control AI-518....24
5.3 DLTS main VI....25

6 Summary & conclusions....26

6.1 Outlook....26

Appendix A....27

References....28

List of figures

Figure 2.1: Silicon crystal....4
Figure 2.2: Bonds in Silicon crystal at T=0K and T>0K....4
Figure 2.3: Band structure for metals, semiconductors & insulators....5
Figure 2.4: The construction of a DLTS signal from the capacitance transients....7
Figure 2.5: The transient starts after the falling edge of the voltage pulse....8
Figure 2.6: Capacitance transient with eight measurement points weighted with three windows of the lock-in function, where Cj is the capacitance value of the j'th point. The windows' value for this particular transient are represented by the symbols to the right of the windows....10
Figure 2.7: A typical DLTS signal with three windows, where the values for each window from the transient in Figure 2.6 are also shown....11
Figure 2.8: Block diagram of a simple VI program....12
Figure 2.9: Front panel of a simple VI program....12
Figure 2.10: LabVIEW functions palette....13
Figure 2.11: Block diagram of a test using GPIB protocol with an external device....14
Figure 2.12: Block diagram of a test using VISA protocol with an external device....15
Figure 3.1: LabVIEW VI hierarchy of the DLTS software....17
Figure 3.2: DLTS software, overview of the front panel in LabVIEW....18
Figure 3.3: Controls of the DLTS software....19
Figure 3.4: The pulse's parameters (Vbias, Vpulse and pulse width), for point 2, 3 and 6. In this thesis Vpulse was chosen to be 5V and Vbias is -5V....20
Figure 3.5: For point 7 & 8, Lock-in function with three windows displaying the minimum window length and relation between the window's lengths. The next following window is always twice as large as the current window....20
Figure 3.6: Two transients, one with the raw data from the CV meter and the other with the signal processed data....21
Figure 3.7: Temperature indicators of the front panel and the STOP button....21
Figure 3.8: The measured capacitance during the bias voltage as a function of temperature....22
Figure 4.1: CV-measurement, capacitance in mF on y-axis and voltage in V on x-axis.23
Figure 4.2: DLTS signal using 6 different lock-in windows (Temperature on the x-axis and DLTS signal on y-axis)....23

List of tables

Table 3.1: Instrument setup....16
Table A.1: NI 488.2/VISA equivalents....27

Abbreviations

C_j	The capacitance of the j'th measurement point, [F]
DLTS	Deep-level transient spectroscopy
DUT	Device Under Test
E_C	Energy level of the bottom of the conduction band (referred to as the conduction band in the text), [eV]
E_g	Forbidden energy range between the E_C and E_V, called bandgap, [eV]
E_V	Energy level of the top of the valence band (referred to as the valence band in the text), [eV]
GPIB	General Purpose Interface Bus
HP	Hewlett Packard
N_i	The number of measurements / measurement points for the i'th window. It is decided by $N_i = 2^i$
S_i	DLTS signal for the i'th window
T	Temperature, [K]
VISA	Virtual Instrument Software Architecture
w_i	The i'th window/weighting function

1 Introduction

Semiconductors are widely used in electronic devices. Their electrical properties are easily controlled and thus they may fit in many different applications. But no electrical device is flawless. For example, when a semiconductor is doped, in order to get some desired property, the semiconductor also obtains some chemical impurities called deep-level defects. The deep-level defects affect the forward and reverse current significantly and increases the noise in transistors. Identification of defects and characterisation of their impact on semiconductors properties is a very important issue since they so radically can change the electrical transport properties of a semiconductor due to thermal heating for example [1].

There is a constant struggle going on to build electronic devices that operate with as small losses as possible. The most fundamental and first step in the construction of an electronic device is the choice of material. One of the most common semiconducting material is silicon and different compounds of silicon, but for more extreme cases, for example where electronic devices are exposed to very high temperatures, a harder material, that can withstand the extreme environment, is needed. Therefore, the interest of using diamond for more extreme electronic applications has increased in the past few years.

Synthetic diamond has been developed for decades, but was not pure enough to be considered for electrical applications. This, however, is not the case today where a new method has made it possible to grow diamond with a small concentration of defects. Because of this, the interest of using diamond for electrical applications has become greater, but, as well as in any other semiconducting materials, there are always some defects present that need to be characterized [2]. In the Division for Electricity at Ångström Laboratory there is an ongoing project focusing on characterizing deep-level defects in synthetic diamond that are situated deep in the bandgap. Such deep levels have a long lifetime and might have a big impact on the electrical properties of diamond devices. The method that is being used is called deep-level transient spectroscopy (DLTS). It is a sensitive quantitative characterization method for deep-level defects.

1.1 Background

In the Division of Electricity the DLTS setup consisted of a C-meter, a pulse generator and a temperature controller. These instruments were controlled with a computer program, which had originally been developed by a Ph.D student at KTH and revised by a research group in Norway. In Norway they had a similar setup to the one here in the Division for Electricity but with some minor differences. The C-meter was the same but the heating controller and the pulse generator were slightly different, hence some changes in the program were necessary.

The program from Norway was created using GPIB communications with the instruments (see section 2.5.1 concerning GPIB). However, when the program was moved to a new computer, the communications stopped working. Since no solution was proposed

to get everything running again the whole project was put aside.

1.2 Assignment

The main purpose of this thesis was to restore the communications between the computer program written in LabVIEW and the instruments and to implement the correct communication syntax with the instruments here in the division of electricity at Ångström. If this was done within the time schedule, further work on DLTS measurement would be possible.

2 Theory

2.1 Atomic- & Band structure in solid-state physics

An atom consists of protons, neutrons and electrons. Each electron occupies different discrete energy levels called orbitals. The outermost occupied orbitals contains the valence electrons which are forming bonds with other atoms and thus create molecules or crystals. To form a molecule, two atoms form a bond with each other by sharing their valence electrons. Silicon for example, which is a common semiconductor, has four valence electrons. When studying a silicon crystal in 2D, a single atom bonds to four neighbouring silicon atoms by sharing each others valence electrons, *see Figure 2.1*.

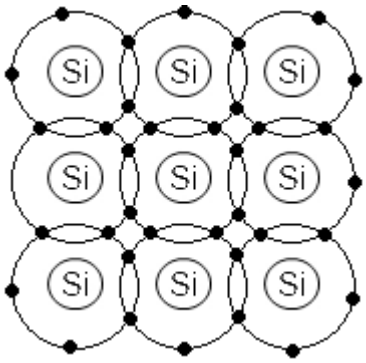

Figure 2.1: Silicon crystal

At 0 degree Kelvin, the valence electrons of silicon are, in some sense, bound to the atom, but at degrees above 0*K* these bonds may be broken due to thermal vibrations, thus causing valence electrons to become free electrons resulting in a hole where the valence electron should have been [3], *see Figure 2.2.*

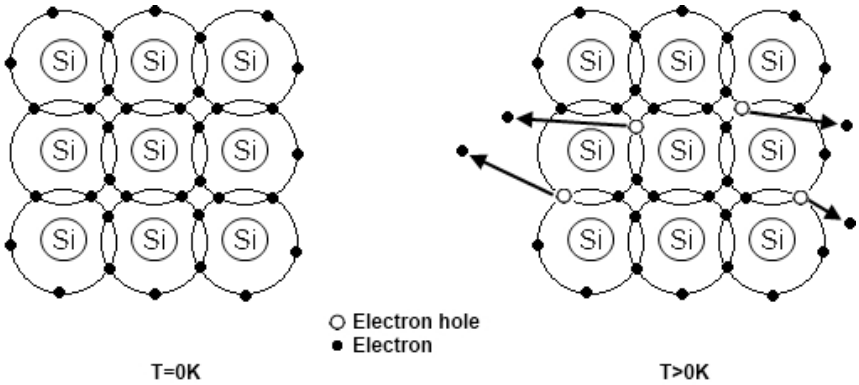

Figure 2.2: Bonds in Silicon crystal at T=0K and T>0K

2.1.1 Valence band & conduction band

In the band theory of solids, the valence band (E_v) is located in the last occupied energy level and contains the valence electrons. The following band, directly above the valence band, is called the conduction band (E_c). In insulators and semiconductors the valence and conduction band are separated by a forbidden energy gap, called bandgap, but in metals they overlap, *see Figure 2.3*. The bandgap (E_g) is referred to as the difference between the valence and conduction band, $E_g = E_C - E_V$ [3].

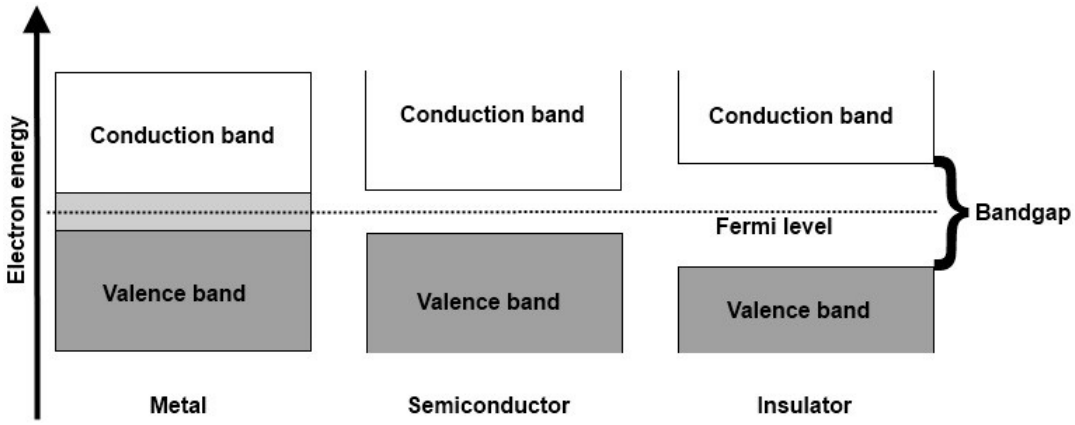

The fermi level, which is drawn in Figure 2.3, has a 50% chance of being occupied by an electron at any given time (assuming thermodynamic equilibrium). In semiconductors, which has the same concentration of electrons and electron holes, the position of the fermi level lies near the middle of the bandgap. If a semiconductor is introduced with impurity atoms, the concentration of electrons versus electron holes changes. This will move the position of E_V and E_C in the energy diagram in Figure 2.3, but the fermi level will be at the same position. Thus, the fermi level will be closer to a band edge, which edge (E_C or E_V) depends on the doping [4]-[5]. This will, of course, change the probability of an electron to occupy the fermi level at any given time.

At $T = 0K$, in a semiconductor, all states in the valence band are occupied and the conduction band is completely empty. At higher temperatures, some of the electrons in the valence band could get enough thermal energy to be excited into the conduction band, thus moving freely within the semiconductor. The vacancy in the valence band is called an “electron hole” and can be regarded as a positively charged carrier.

2.2 Defects

To control the electronic properties of a semiconductor, such as conductivity and conductivity type (n- or p-type), impurity atoms are introduced into the semiconductor material, this process is called doping. One, quite accurate and often used, technique is

ion implantation, by which ions are accelerated in an electric field and impacted into a solid. However, this method will also cause creation of deep-level defects [6].

Defects can be classified as “shallow” or “deep” depending on their position relative the valence and conduction band edge. Shallow defects have allowed energy states close to the edges and deep-level defects closer to the middle of the bandgap [6]-[7].

2.2.1 Deep-level defects

Deep-level defects are the product of chemical impurities and strongly intervene with the electrical and atomic transport properties of semiconductors [1]. They also increase the noise in photodiodes and transistors and reduce the minority carrier lifetime [8].

2.2.2 Traps

The majority charge carriers in a n-type semiconductor are electrons and the minority carriers are holes, while in p-type semiconductors it is the opposite. If a carrier spends a relatively long time at the defect it is said to be trapped. A trap captures either electrons or holes, it is highly unlikely for it to capture both [7].

2.3 Deep-Level Transient Spectroscopy

Deep-Level Transient Spectroscopy (DLTS) is a method to detect deep-level defects in a semiconductor. The method was first introduced by D.V. Lang, who obtained a DLTS signal simply by measuring the difference of two capacitance values at two fixed times during the transient [9]. This method is called *boxcar* and is illustrated in Figure 2.4.

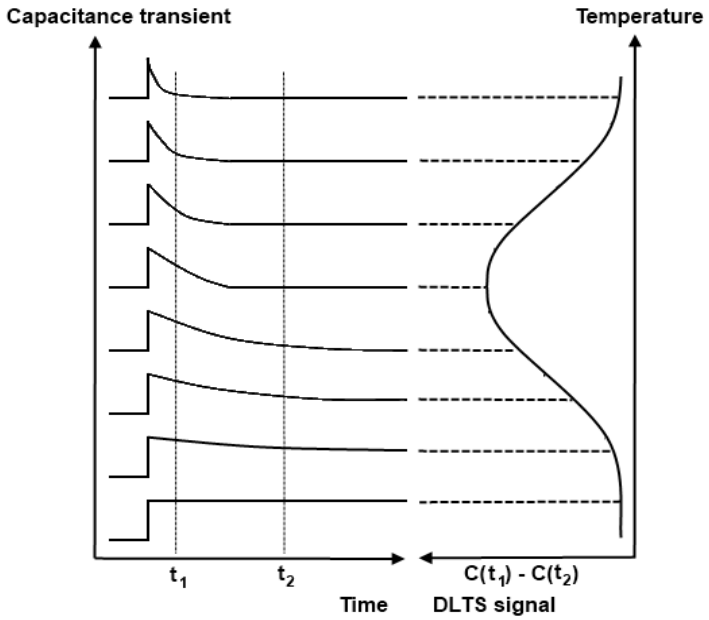

Figure 2.4: The construction of a DLTS signal from the capacitance transients

Figure 2.4 shows two plots: eight different transients with different time constants to the left and to the right is the corresponding DLTS signal the transients give rise to. By calculating the difference in capacitance for time t_1 and t_2 of each transient, the DLTS signal can be obtained.

Nowadays the technique has been refined, yet keeping the basics of Lang's method unchanged [9]. By measuring the capacitance transient of the sample for different temperatures and multiply it with a weighting function, the DLTS signal is obtained through the integration of that product [10].

2.3.1 The capacitance transient

The purpose of DLTS is to characterize the deep-level defects in the samples. This is done by measuring capacitance transients. The influence of deep-level defects on the capacitance of the device under test (DUT) is as follows: The capacitance of the semiconductor's *space-charge region* (the region of the semiconductor which is free of mobile charge carriers, also called *depletion region*) depends on the space-charge concentration. Space-charges are fixed charges such as impurity ions or electrically charged deep-level defects. The deep-level defects can trap mobile charge carriers and therefore change the space-charge concentration. The lifetime τ of a trapped charge carrier is proportional to $\exp(\Delta E / k_B T)$, such that the re-emission becomes more likely for higher temperature T and less likely for traps deep in the bandgap: $\Delta E \approx E_g / 2$. So if the total trap concentration is N_T and all traps are filled at time t=0, the concentration of filled traps for $t > 0$, if re-trapping is neglected, is given by Eq. 2.1.

$$n_T = N_T \cdot \exp\left(\frac{-t}{\tau}\right) \tag{2.1}$$

Since the *trapped* charge concentration changes with time, it will give rise to a time-dependent *space*-charge concentration and therefore a time-dependent capacitance. This capacitance is referred to as the transient and can be obtained by applying a voltage across the sample (DUT), as shown in Figure 2.5.

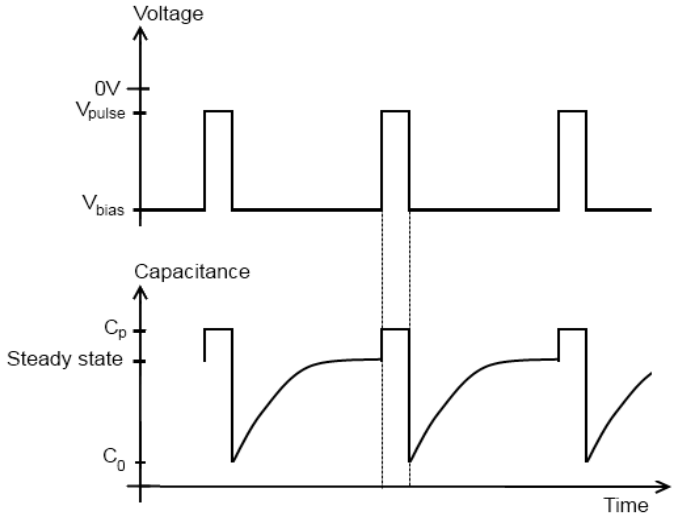

Figure 2.5: The transient starts after the falling edge of the voltage pulse

In a n-type semiconductor, the approach is to provide enough thermal energy to the sample so that the captured electrons in possible existing traps can get enough energy to be emitted. The technique is to apply a reversed bias voltage across the sample in order to empty the traps of all electrons that have received enough thermal energy to be able to be emitted. Then, a short forward pulse, filling pulse, is applied, of a magnitude that makes it possible for the traps to recapture the electrons. The pulse is withdrawn and the bias is again applied. At this point, the transient is at its beginning and will change over time with proportion to the emission of the trapped electrons. This process is done multiple times for each temperature and the transient is averaged to reduce possible noise.

The process can be associated with that of a simple parallel plate capacitor. During the filling pulse, the distance between the capacitor's plates decreases and the capacitance increases. With the reversed bias, one can imagine that the distance between the plates has increased, causing the capacitance to decrease. But, at this point, the emission of the trapped electrons takes place and will cause the capacitance to successively increase with time.

2.3.2 Window & weighting functions

Windowing is a method used for observation of a mathematical function within a certain time interval. The windowed function is obtained by multiplying the function of obser-

vation with a weighting function, that has a given shape and amplitude within the interval but is zero outside. In some sense, it can be recognized as a filter. There are many different types of weighting functions, all giving slightly different results of shape and quality of the windowed function.

One example is the *lock-in* function, $w_i(t)$, which is basically a rectangular signal and is given by Eq. 2.2.

$$w_i(t) = \left\{ \begin{array}{rl} -1 & : \; 0 < t < \frac{t_i}{2} \\ 1 & : \; \frac{t_i}{2} < t < t_i \\ 0 & : \; otherwise \end{array} \right\} \tag{2.2}$$

2.3.3 DLTS signal

For discrete time, the DLTS signal can be described with eq. 2.3, where $w_i(t)$ is the window i, N_i is the number of measurements for window i and $C_j = C(t_j)$ is the capacitance value of the j'th measurement point at $t = t_j$. The number of measurement points for window i is decided by $N_i = 2^i$.

$$S_i = \frac{1}{N_i} \sum_{j=1}^{N_i} C_j w_i(t) \tag{2.3}$$

By inserting eq. 2.2 in eq. 2.3 it can be rewritten as:

$$S_i = \frac{1}{N_i} \left[\sum_{j=N_i/2+1}^{N_i} C_j - \sum_{j=1}^{N_i/2} C_j \right] \tag{2.4}$$

To obtain the DLTS signal, the lock-in function is used with the transient as shown in Figure 2.6. The figure only shows one step and will result in one point per window of the DLTS signal. In order to get a spectrum this is done for multiple temperatures.

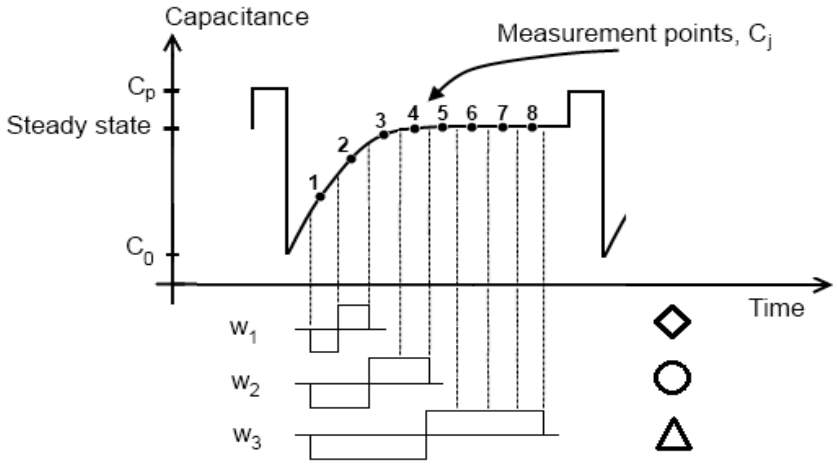

There are three lock-in signals used in Figure 2.6. The windows are using eight measurement points of the capacitance transient and the first window, w_1, locks only two measurement points, w_2 locks four and w_3 locks eight. With eq. 2.4 the DLTS signal's value of w_1, w_2 and w_3 can be calculated as

$$S_1 = \sum_{j=2}^{2} C_j - \sum_{j=1}^{1} C_j = C_2 - C_1$$

$$S_2 = C_4 + C_3 - C_2 - C_1$$

$$S_3 = C_8 + C_7 + C_6 + C_5 - C_4 - C_3 - C_2 - C_1$$

The transient in Figure 2.6 will be a value around the peak of the DLTS signal for w_2 as shown in Figure 2.7, where the whole spectrum is illustrated.

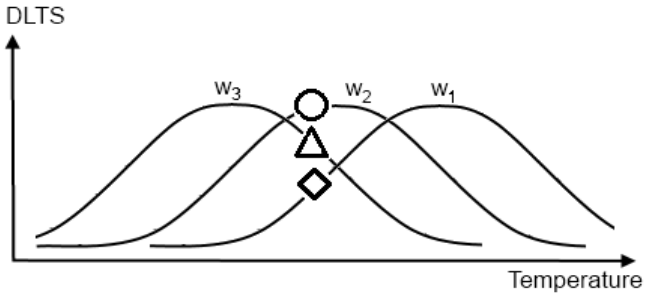

Figure 2.7: A typical DLTS signal with three windows, where the values for each window from the transient in Figure 2.6 are also shown.

The usage of windows makes it possible to study all different shapes of the transient. For faster increasing (decreasing) transients, a narrow window will give rise to a peak of the DLTS signal and for slow transients, a wide window is needed.

2.4 Analysis of DLTS & Arrhenius plot

Each deep-level defect gives rise to a peak in the deep-level transient spectrum and the height of the peak is proportional to the defect concentration. From the peak it is also possible to determine the energy position in the bandgap and the carrier capture cross section. This is done with an Arrhenius plot, which will result in a straight line of which the activation energy can be extracted from the slope and the carrier capture cross section from the intersection of the line with the y-axis [11]. (For further research in this subject see chapter 4 of *Capacitance Transient Measurements on Point Defects in Silicon and Silicon Carbide* by H. Kortegaard Nielsen).

2.5 LabVIEW

LabVIEW (Laboratory Virtual Instrument Engineering Workbench) is a graphical programming environment from National Instruments (NI). It is a tool for easy communication with, and development of measurement and control systems for, external hardware. The user creates so called Virtual Instrument (VI) blocks to obtain the wanted functionality. LabVIEW is created so that a VI consists of a block diagram, which contains the source code, and a front panel, which basically is the user interface where the user can display the results and, sometimes, controlling the functionality of the VI.

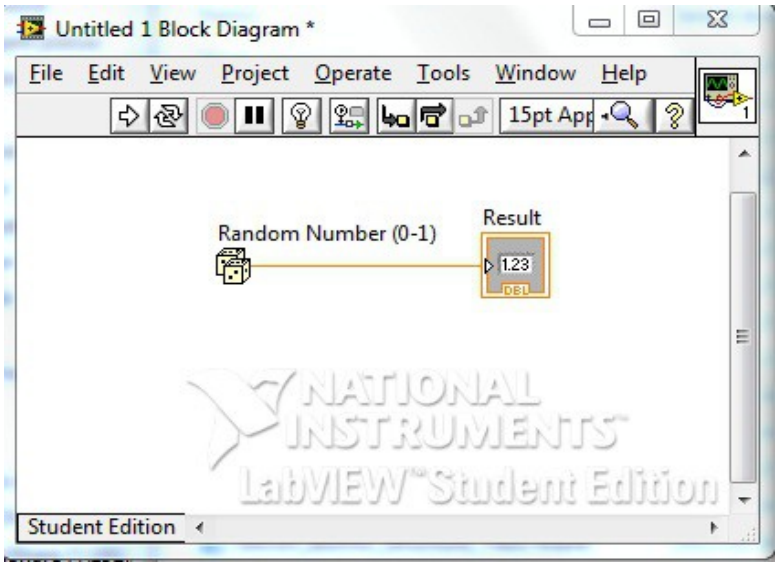

In Figure 2.8 the block diagram of a simple VI is illustrated. It contains a built-in function that generates a random number and send the result through the wire to an indicator labelled *Result*. The result is not shown in the block diagram, instead it is shown in the front panel where the indicator automatically has been placed when adding it to the block diagram, as shown in Figure 2.9. To run the program the user simply pushes the arrow in the top left corner of the window, either in the block diagram or in the front panel.

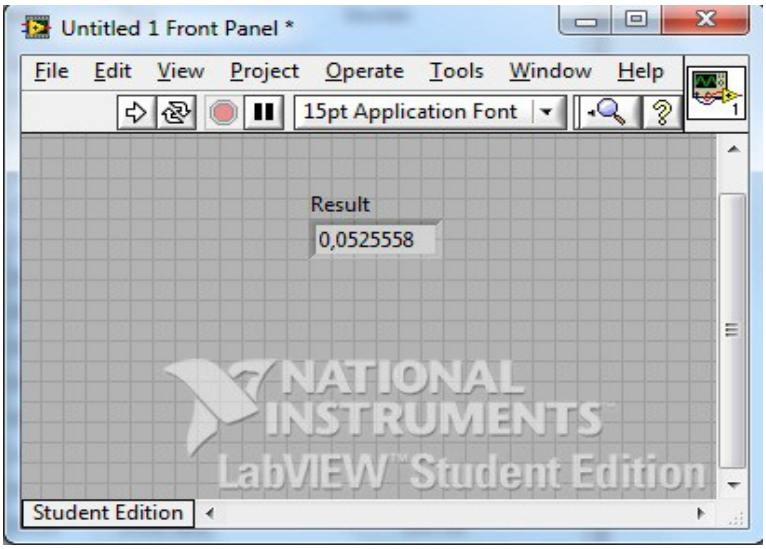

A VI is made with different components and/or sub-VI's wired together in the block diagram in a manner of the users choice. One example of components are standard mathematical operations such as multiplier, adder etc. For more advanced mathematics and programming there are predefined sub-VI's integrated in LabVIEW. All sub-VI's and components are accessed through the LabVIEW functions palette, which is show in Figure 2.10.

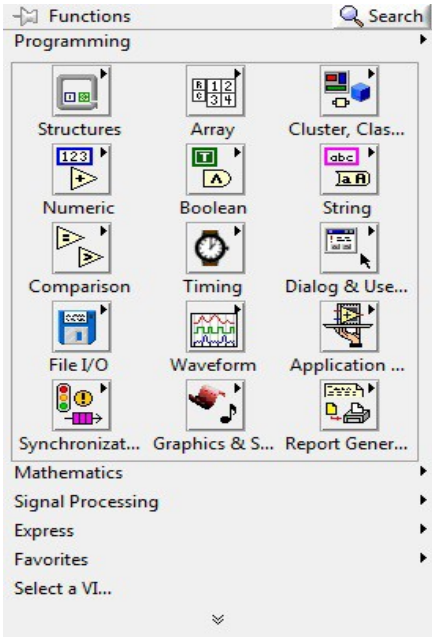

Figure 2.10: LabVIEW functions palette

If a certain desired function does not exist in the palette the user can construct their own sub-VI with the function and add it to the palette for easy access. When creating larger VI's the use of sub-VI's is a great tool for hiding low level functions in the block diagram, thus creating hierarchies with a main VI in the top.

2.5.1 VISA/GPIB

Virtual Instrument Software Architecture (VISA) is a protocol used for communication between a PC and external hardware. It includes serial communication through COM ports and more specific I/O interfaces such as IEEE-488, or commonly known as General Purpose Interface Bus (GPIB), which was developed by Hewlett Packard for easier interconnection with their instruments. In LabVIEW there are sub-VI's for both VISA and GPIB protocols. It is mostly up to the user which one to choose, since VISA includes GPIB communication as well, compare Figure 2.11 with Figure 2.12. However, in National Instruments' NI-VISA user manual, they recommend using VISA sub-VI's for the entire system when programming multiple devices that communicate over more than one bus-type [12]. Even Agilent technologies states on their website that it would be better to use the more general VISA protocol instead of GPIB protocol.

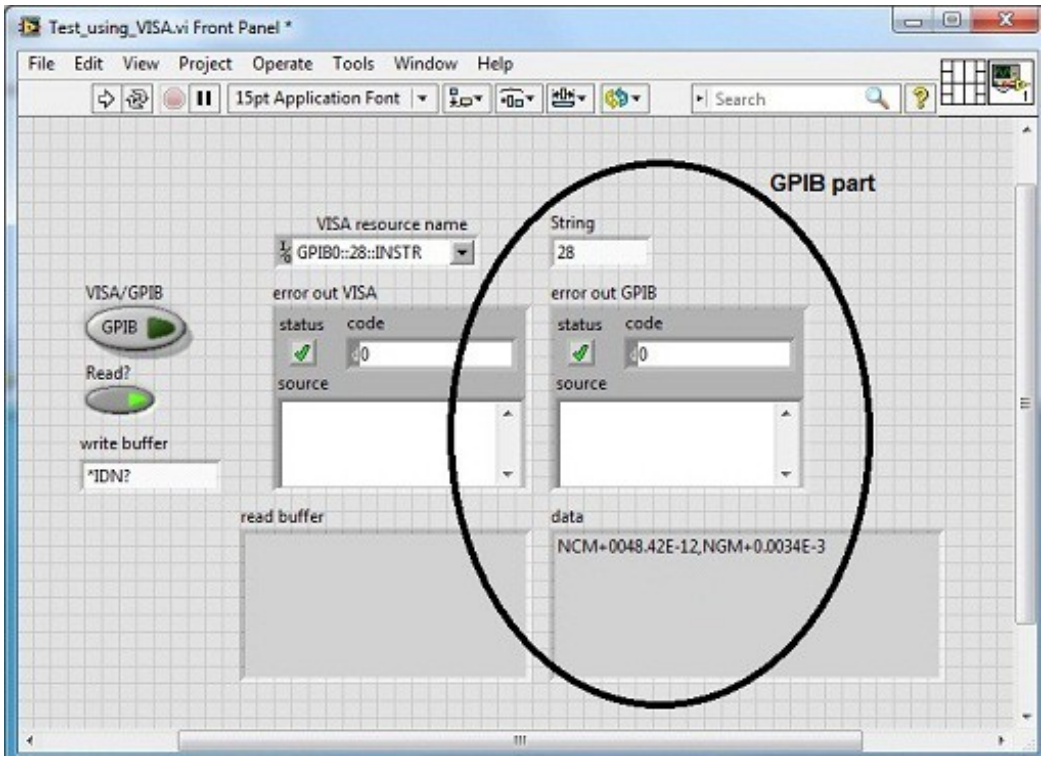

In Figure 2.11 the standard command *IDN? is sent to an external device using GPIB protocol in LabVIEW and the response is read as a string shown in the box labelled *data*. The *IDN?-command asks the targeted device for its identity and the response string in this case contains information about the capacitance and conductance.

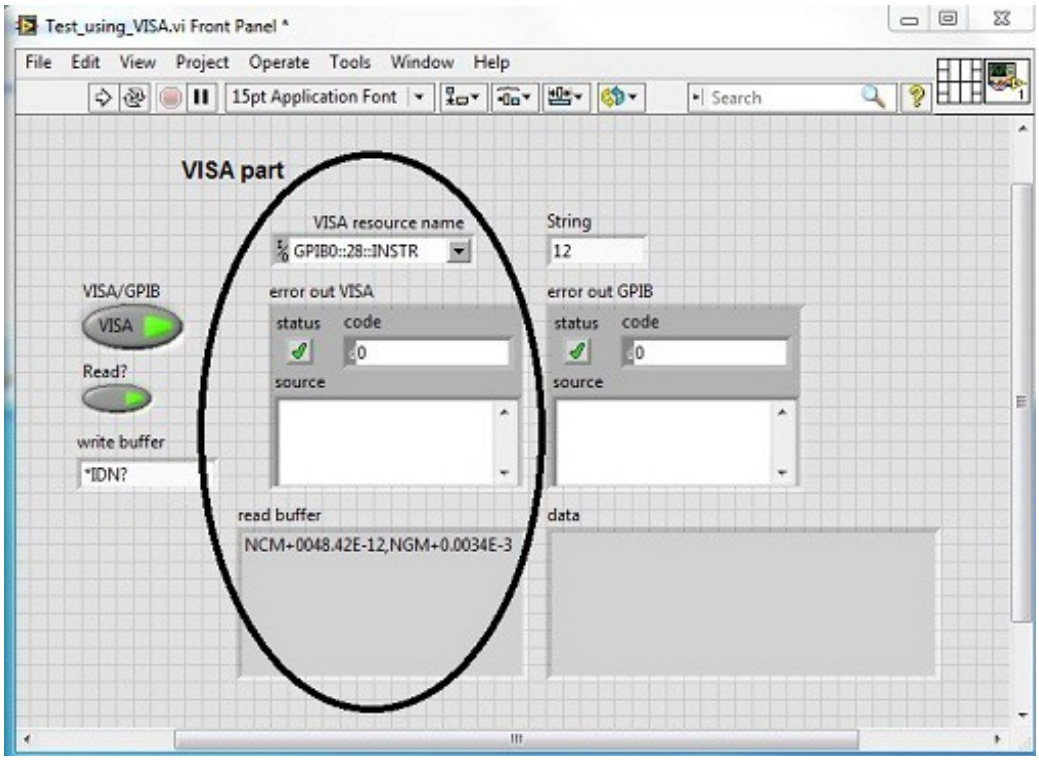

In Figure 2.12 the same command is sent to the same device as in Figure 2.11, but instead with VISA protocol in LabVIEW and the response is exactly the same. The conclusion of this is that even though the external devices is connected with GPIB buses to the PC, LabVIEW still can handle this with VISA VI's. What is expected, since VISA contains GPIB communication.

3 Method

3.1 Experimental setup

The instruments that were used in the experiments are listed in Table 3.1.

Device	Model
C-meter / C-V plotter	HP 4280A
Pulse generator	HP 8112A
Temperature controller	Tectra HC 3500 with Yudian AI 518P (Programmable artificial intelligent temperature controller)

The C-meter was used to measure the capacitance across the sample, the pulse generator controlled the voltage pulses and with the temperature controller the temperature was controlled and measured at the sample. The pulse generator and the C-meter was connected together in order to synchronize the measurements, so that no pulses was applied across the sample during a capacitance read and no read of the capacitance was made during a voltage pulse.

In order to control the instruments, they were all connected to a PC, on which a LabVIEW program had been constructed to perform DLTS measurements and collect data. The DLTS control program had been built by a research group in Norway. Since they were using another type of pulse generator and temperature controller which meant that the control commands of those instruments were different and needed to be adjusted in the LabVIEW program to fit the instruments at Ångström Laboratory. For the Yudian controller a number of VI's had been created by the research group at Ångstöm Laboratory that contained most of the commands and functions needed for the DLTS main program.

Figure 3.1 shows the hierarchy of the DLTS software with the main VI on top and its sub-VI's below. The box at the bottom to the right contains the library of driver VI's for Yudian's temperature controller.

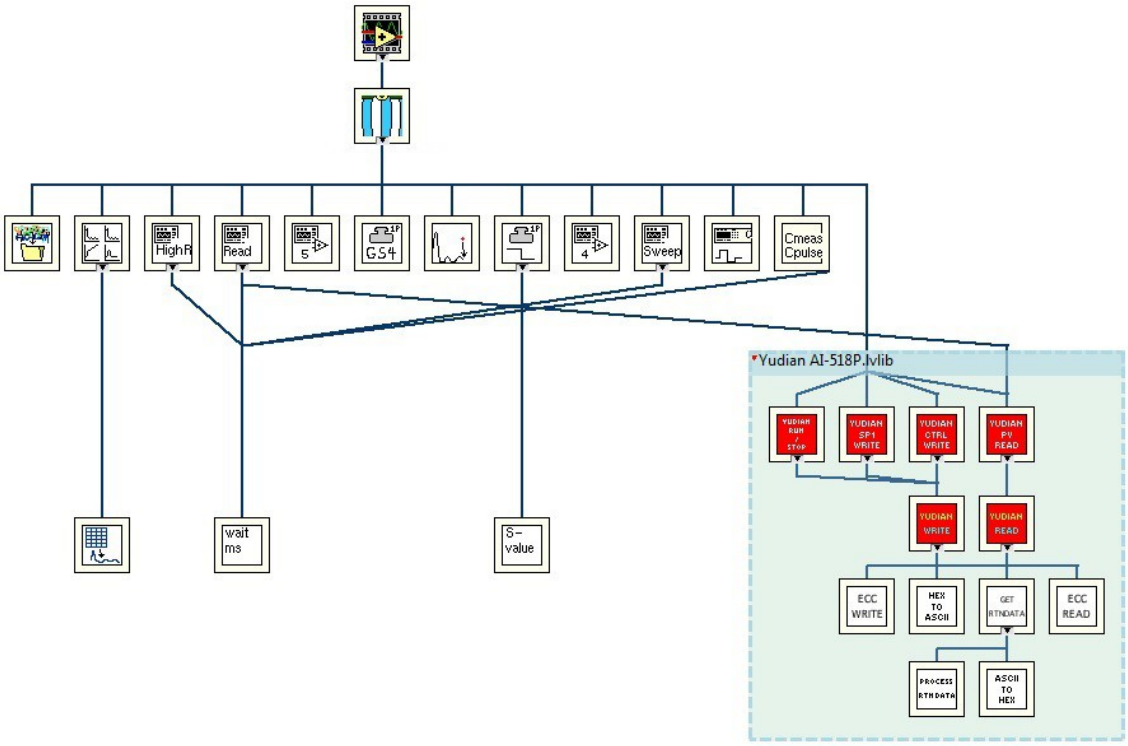

A detailed description of most of the VI's in Figure 3.1, except the driver library for Yudian's temperature controller, can be found in *A LabVIEW program for Deep-level transient spectroscopy*, by W. Liu [6].

3.2 Implementation

The front panel of the DLTS software is displayed in Figure 3.2 in which the following parts are marked by circles:

A. The controls of the settings to initialize a measurement.

B. The path of the save file in which the measurement data is stored.

C. The indicators that displays the results of the measurements and the stop button.

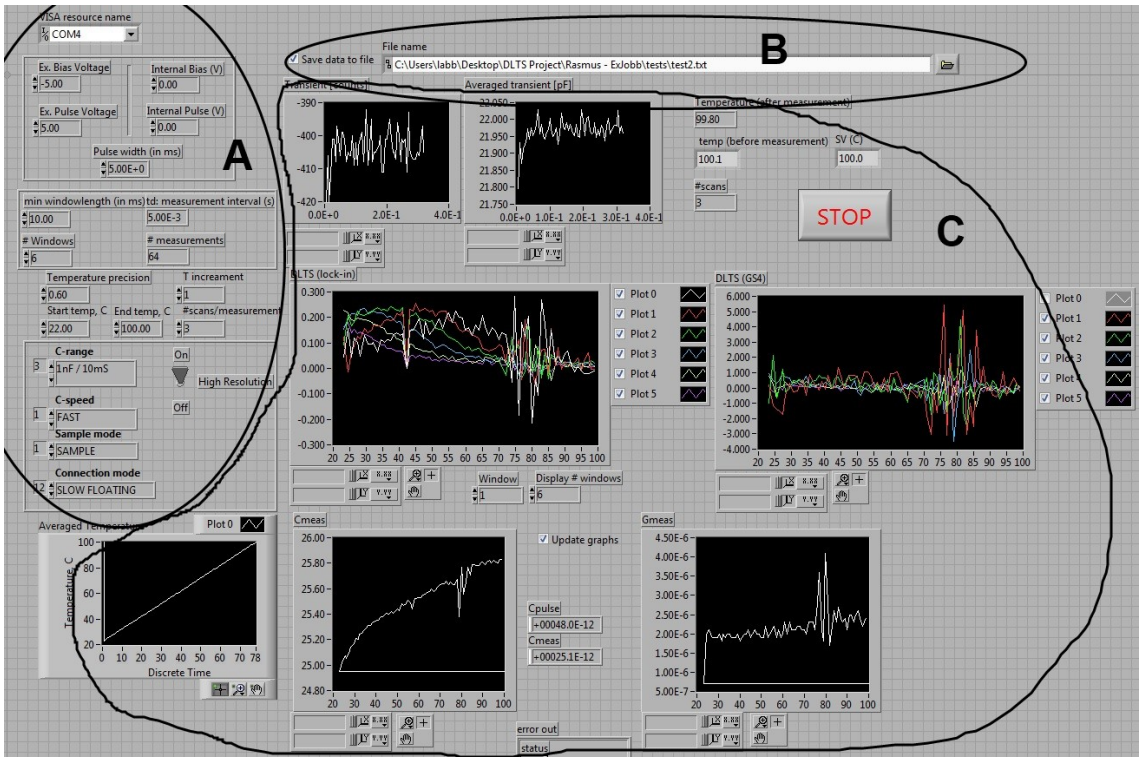

3.2.1 Controls

The controls, shown in region A of Figure 3.2, are set before running the VI, because when pushing *run*, the program reads the values of the controls and initializes the measurement with these settings. Of course, if anything goes wrong the stop button would abort the program when pushed.

A closer view of the controls on the front panel is shown in Figure 3.3.

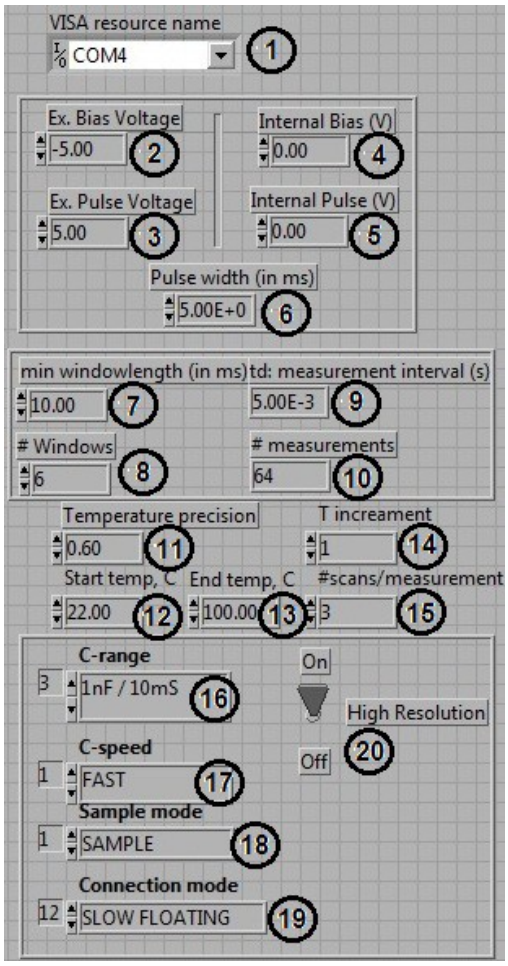

Figure 3.3: Controls of the DLTS software

1 This specifies the COM-port to which the temperature control is connected.

2 Sets the pulse generator's bias voltage, see Figure 3.4.

3 Sets the pulse generator's pulse voltage, see Figure 3.4.

4 When using an internal pulse set by the C-meter this sets the bias voltage.

5 When using an internal pulse set by the C-meter this sets the pulse voltage.

6 Sets the pulse width in ms, see Figure 3.4.

7 Minimum window length, in ms, sets the first window's length, the next window has automatically the double length of the previous window, see Figure 3.5.

8 Sets the number of windows, see Figure 3.5.

9 This one is an indicator related to 7 It is not controllable by the user, instead it gets the value that is half of the min windowlength.

10 An indicator showing two to the power of number of windows.

11 This sets the accuracy of the temperature at which a measurement can be made. This relates to how well the PID parameters are set in the temperature controller, i.e. a measurement is started when the temperature is within the interval of [T-Temperature precision/2, T+ Temperature precision/2].

12 Start temp: the first temperature at which a measurement is made.

13 End temp: the last temperature at which a measurement is made.

14 Sets the increment step of the temperature.

15 Sets the number of scans per measurement, i.e. the number of scans per temperature. A measurement at a temperature is averaged over the number of scans in order to reduce noise.

16 C-range is only active in the program when high resolution (20) is OFF. It tells the C-meter in what range the capacitance is expected to be measured within. If it is chosen too low, an overflow will occur and the data will be invalid. However, choosing a high value will reduce the accuracy of the measurement data.

17 C-speed specifies if the measurement of the capacitance is to be made in *fast mode* or *slow mode*. As the names suggests *fast mode* provides optimum speed but also less accuracy compared to *slow mode*.

18 Specifies the sample mode of how the C-meter will perform the data collection of a measurement, In BURST mode the 4280A makes one measurement per measurement point. In SAMPLE mode, however, it repeats several partial measurements at each measurement point.

19 This specifies the connection mode between the C-meter, the DUT and the external pulse generator, i.e. to which one of the inputs, *slow* or *fast*, the pulse generator's output is connected and how the DUT is grounded.

20 With high resolution ON the capacitance is related to a capacitance offset, measured while in steady-state (the capacitance across the sample, with bias voltage applied, after the transient has converged and become stable). When OFF the offset is set to zero.

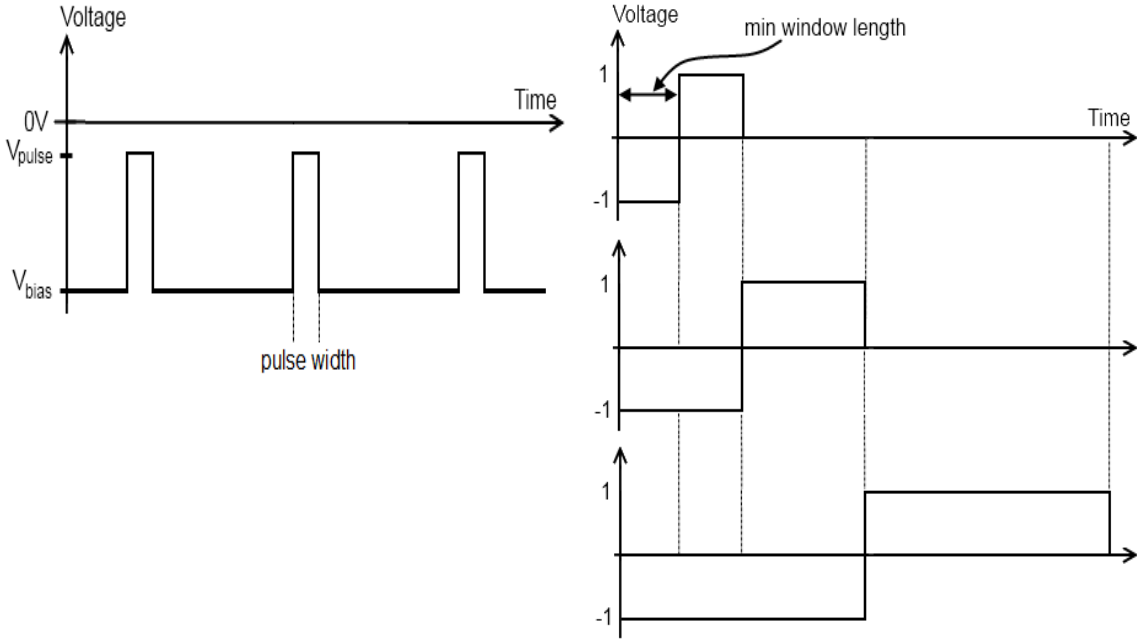

Figure 3.5: For point 7 & 8, Lock-in function with three windows displaying the minimum window length and relation between the window's lengths. The next following window is always twice as large as the current window.

3.2.2 Indicators

The indicators of the front panel are located in region C of Figure 3.2. Here follows a description of some of the indicators.

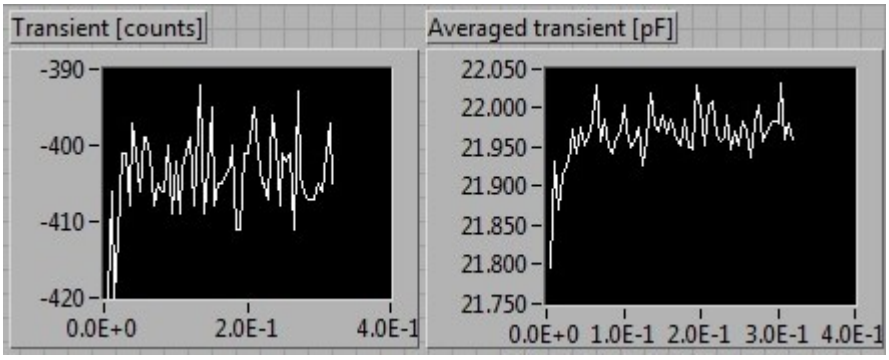

The left transient of Figure 3.6 consists of raw data, called *counts*. It is the measured capacitance in binary coded format. Together with this data from the CV meter a status byte is sent, which contains information of how to convert the capacitance data into values represented in Farads. In the right transient the raw data has been converted into representation of pF.

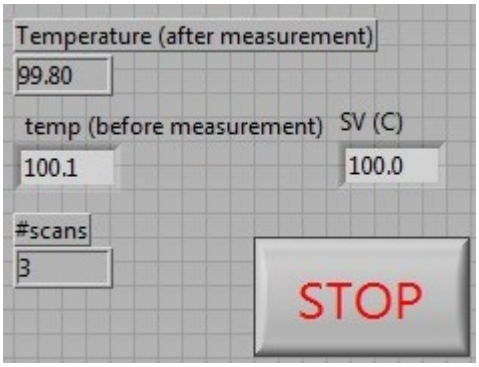

Figure 3.7: Temperature indicators of the front panel and the STOP button

The content of Figure 3.7 can be found to the right of the transient indicators in the front panel. It displays the SV (C), which is the set value of the temperature controller in degrees Celsius. Since the current temperature varied due to a bad PID parameter choice of the temperature controller, it was interesting to see what the temperature was before and after the measurement so that an understanding of how well the measurement was made at wanted temperature could be done. In the figure the *STOP* button could also be found, which aborts the program and finishes the current measurement at any point.

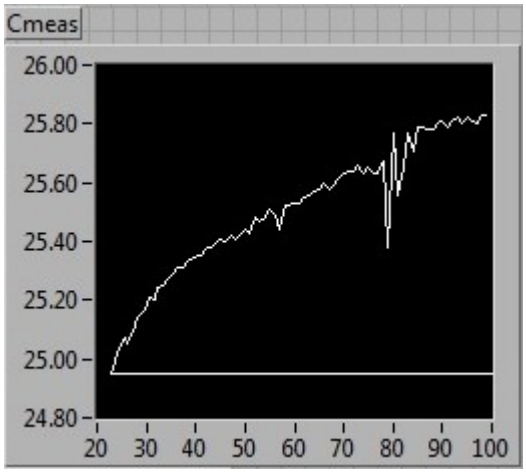

Figure 3.8: The measured capacitance during the bias voltage as a function of temperature

Figure 3.8 displays the steady-state capacitance, measured with a fixed reverse bias, V_{bias}, applied, at each temperature. Next to this indicator, to the right on the front panel, is the measured conductance during the bias voltage (see Figure 3.2).

There are also indicators in the front panel which plots the DLTS signals using lock-in and GS4 (which is not described in this thesis) weighting functions.

4 Results

After the basic GPIB communication VI's had been replaced with VISA a successful CV-measurement was made and is shown in Figure 4.1.

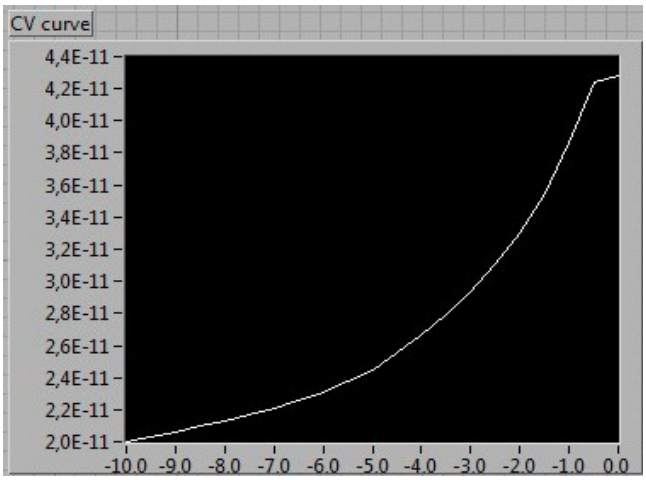

The measurement was made by sweeping a reverse voltage from 0V to -10V and measure the capacitance of the sample at room temperature. When applying a reverse voltage across the sample the depletion region was expanded and the capacitance decreased with proportion to the decreasing voltage as seen in Figure 4.1.

At the final step of this thesis a fully successful DLTS measurement was made using six lock-in windows at 25ºC to 100ºC and is shown in Figure 4.2.

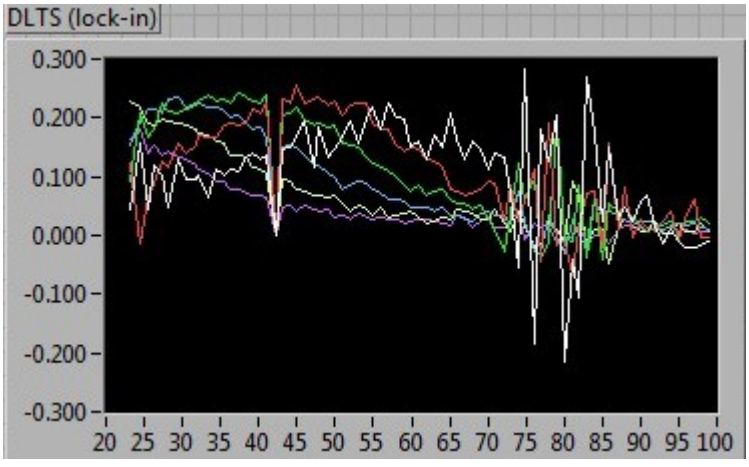

5 Discussion & Analysis

5.1 Communications

The first problem to solve was to understand why the communication with the devices did not work. The only time they gave a response was when using NI MAX's VISA test panel, which allowed the user to send simple commands to the connected device in order to see if it responded. Since the VISA test panel used standard VISA commands to write and read to the device, the problem seemed to be the GPIB VI's in the LabVIEW programs. All the GPIB VI's were then replaced with VISA VI's instead, according to Table A.1 in Appendix A, and the connected devices now gave responses even in LabVIEW. A successful CV measurement was then made at room temperature in order to see that everything worked properly with the C-meter.

Later it was discovered that the GPIB card in the PC from Agilent technologies was not compatible by default with National Instruments NI-488.2 protocol. But Agilent tech. provided a configuration for enabling communication with NI-488.2 through their program Agilent Connection Expert that are included in Agilent IO Libraries Suite 16.3. When enabling this, the GPIB VI's in LabVIEW started to work. Nevertheless VISA VI's were still chosen to be used due to the recommendations from NI and Agilent and the fact that it would be much easier to replace one of the instrument if the replacement were using another type of communication.

5.2 Yudian control AI-518

The next step was to understand the heater and why it did not work in the DLTS program. The communication with the Yudian controller was made through a USB to serial adapter and therefore VISA VI's had to be used in LabVIEW. The first thing that was added to the existing VI's for Yudian in the DLTS main program was a VISA CLOSE function at the end of each VI's execution to properly close the opened session for that port. If the port is not closed it stays open for the task it was opened for and locked for other uses. When this was done the communications with Yudian worked quite well.

However when a value was sent to Yudian to set a parameter, the answer could sometimes be ten times larger or ten times less than the wanted value. This was no fault, merely an effect of how the Yudian controller was programmed to read and write data. According to the datasheet of Yudian the response of all parameters with the same unit as PV (process value) had to be divided by 10, when the dPt (decimal point) was set to '1' or higher, in order to show the correct value. Also noticeable is that the written value to a parameter with the same unit as PV had to be multiplied with 10 before sent to the Yudian control to get the desired value correctly set. Just to make sure, most of the parameters were tested and processed accordingly so that it became user friendly, i.e. if the user sent 10 to SP1 (setpoint 1), the Yudian control would interpret it as 10 and set SP1

to the same value.

All these changes led to quite a number of backup files and different versions of the Yudian VI's. They were scattered in different directories on the computer which made LabVIEW lose track of the ones that really mattered. Therefore, it was decided to collect the working and updated versions in a user specified driver and add it in the LabVIEW palette for easy access whenever needed, thus preventing LabVIEW to link a sub-VI to the wrong VI.

Later it was discovered that there were some values of some parameters that could not be read in LabVIEW. Yudian did write the value correctly to the specified parameter, but when trying to do a read of the same parameter value the answer from Yudian could not be recognized as a true value by the computer. It was discovered that the received binary bytes from Yudian sometimes contained the same value as what the termination character of the port was set to represent. This meant that when LabVIEW encountered the value representing the termination character, LabVIEW thought that the reading was done and therefore ended it, thus skipping the rest of the bytes. Realizing this, the solution was to disable the termination character and to change the property "Serial End Modes for Reads" from default to "None(0)", which meant that the read would not stop when the termination character was encountered.

5.3 DLTS main VI

When all this was done, the Yudian VI's worked properly and put as a driver in the LabVIEW palette, it was time to see to the main DLTS VI. Since it originally came from a group in Norway, who used a different setup with different brands and models for their devices, some changes needed to be done in the main VI. It concerned the changing of the instrument commands to the corresponding ones that could be applied to this setup.

When the commands had been changed, another problem was revealed. The Operating System used by the computer was using Swedish standards, thus using a comma for decimal mark, not point as of the English standard. This lead to parsing errors in the devices, that used the English standard. By adding a format string in LabVIEW to every written command the decimal mark was changed to be a point instead of a comma, but just to make sure that every value in LabVIEW used point and not comma the change were also made in the OS.

6 Summary & conclusions

Both NI and Agilent technologies recommend the users of GPIB and 488 protocols to change to using the VISA protocol instead. The reason for this is, according to Agilent's website, that Agilent 488 and NI-488.2 is proprietary libraries. Another reason would be that it makes the program much more generalized. For example if a device is replaced for one with another brand/model and the new uses another type of communication, it will be much easier to make the change if the program is written using VISA VI's rather than GPIB. Because, then the only thing that needs to be changed is the addresses of the ports that are being used and perhaps correct the commands that is sent to the device.

As of this the main purpose of this thesis, to get the communication between LabVIEW and the external instruments to work, was achieved and proved with the CV measurement, in Figure 4.1, and the DLTS measurement, in Figure 4.2.

6.1 Outlook

As for the future there are still some work with the DLTS software and making it more user-friendly. A lot of the things can be updated in order simplify the code and make it more effective. As for example wait until the temperature controller has reached and is stable at its set point before entering the measurement loops. As well as remove the high/low resolution choice and other controls that are not in use with the current setup, so that no one gets confused about them being in the front panel. Or at least set them as a constant in the block diagram in case if any of the instruments being replaced and the controls then would be useful.

The hardware settings could also be considered for improvement. The PID parameters of the temperature controller for example, could be better chosen in order to stabilize the regulation and get it more accurate.

Other things that could be done is to implement more data acquisition functions such as depth profiling and Arrhenius plots in order to analyse the results more easily. Even a FAQ or manual could be most appropriate for future work and troubleshooting.

Appendix A

C NI-488 Device Function	C VISA INSTR Operation	LabVIEW NI-488 Device Function	LabVIEW VISA INSTR Operation
ibdev	viOpen	<no equivalent>	VISA Open
ibonl	viClose	<no equivalent>	VISA Close
ibwrt	viWrite	GPIB Write	VISA Write
ibrd	viRead	GPIB Read	VISA Read
ibclr	viClear	GPIB Clear	VISA Clear
ibtrg	viAssertTrigger	GPIB Trigger	VISA Assert Trigger
ibrsp	viReadSTB	GPIB Serial Poll	VISA Read STB
ibwait	viWaitOnEvent	Wait for GPIB RQS	Wait for RQS
ibconfig	viSetAttribute	GPIB Initialization	VISA Property Node

References

[1] H. J. von Bardeleben, J. C. Bourgoin, D. Deresmes, A. Huber and D. Stievenard, *Identification of a defect in a semiconductor*, Phys. Rev. B 34, 7192 (1986)

[2] J. Isberg, et al. "*High carrier mobility in single-crystal plasma-deposited diamond*." *Science* 297.5587 (2002): 1670-1672.

[3] J-P. Colinge & C. A. Coolinge, *Physics of Semiconductor Devices*, Print ISBN: 1-4020-7018-7, eBook ISBN: 0-306-47622-3, (2002).

[4] S. M. Sze, *Physics of Semiconductor Devices,* ISBN 0-471-05661-8. Wiley. (1964)

[5] C. Kittel, *Introduction to solid state physics*, 7th edition, ISBN 0-471-11181-3. Wiley. (1996)

[6] W. Liu, Master of Science Thesis: *A LabVIEW program for Deep-level transient spectroscopy*, KTH, Stockholm (2009)

[7] S. Majdi, Master Thesis: *Deep level transient spectroscopy investigation of silicon carbide diodes*, KTH, Stockholm (2005)

[8] B. Schumacher, H-G. Bach, P. Spitzer, J. Obrzut, Chapter 9: *Electrical Properties* in *Springer Handbook of Materials Measurement Methods*, ISBN 978-3-540-20785-6. Springer-Verlag Berlin Heidelberg, 2006, p. 431

[9] P. Pellegrino, Ph.D thesis: *Point defects in ion-implanted silicon and silicon carbide*, KTH, Stockholm (2001).

[10] D. Åberg. Ph.D thesis: *Capacitance Spectroscopy of Point Defects in Silicon and Silicon Carbide*, KTH, Stockholm (2001).

[11] H. Kortegaard Nielsen, Ph.D thesis: *Capacitance Transient Measurements on Point Defects in Silicon and Silicon Carbide*, KTH, Stockholm (2005).

[12] VISA: NI-VISA user manual, 1996 (2001 edition), National Instruments Corporation.